Nuclear Materials and Energy 9 (2016) 465–470

Contents lists available at ScienceDirect

Nuclear Materials and Energy

journal homepage: www.elsevier.com/locate/nme

The influence of carbon on the resistivity recovery of proton irradiated Fe–11 at.% Cr alloys

G. Apostolopoulos[a,*], V. Lukianova[a], Z. Kotsina[b,a], A. Lagoyannis[c], K. Mergia[a], S. Harissopoulos[c], S. Messoloras[a]

[a] Institute of Nuclear & Radiological Sciences & Technology, Energy & Safety, N.C.S.R. "Demokritos", GR-153 10 Aghia Paraskevi, Greece
[b] Department of Solid State Physics, Faculty of Physics, National and Kapodistrian University of Athens, Panepistimioupolis, GR-157 72 Athens, Greece
[c] TANDEM Accelerator Laboratory, Institute of Nuclear & Particle Physics, N.C.S.R. "Demokritos", GR-153 10 Aghia Paraskevi, Greece

ARTICLE INFO

Article history:
Available online 28 September 2016

Keywords:
Resistivity recovery
Point defects
Carbon
Fe–Cr alloys
Proton irradiation

ABSTRACT

The effect of carbon on the point defect migration properties in Fe–Cr alloys with a concentration of 11 at.% Cr is studied by means of resistivity recovery measurements after low temperature proton irradiation. The presence of carbon mainly affects features of the resistivity recovery spectra in the temperature ranges of (a) 150–200 K, which are linked to self-interstitial defects, and (b) 400–500 K, which are probably due to vacancy and vacancy-carbon complexes. The experimental results are discussed in terms of the possible interactions of carbon with radiation defects and its influence on solute atom re-ordering.

1. Introduction

Carbon is one of the most important alloying elements in steels playing a key role in the development of the microstructure and the mechanical properties. It has also a major influence on the irradiation behavior due to its strong interaction with point defects. A number of experimental [1,2] as well as theoretical [3,4] works have demonstrated the strong influence of carbon impurities on the migration and annealing of point defects in iron. It has been shown that the formation of carbon-vacancy complexes is energetically favorable and, moreover, these complexes exhibit reduced mobility and may serve as nucleation sites for larger vacancy clusters and nanovoids. The interaction between carbon and self-interstitial atoms is also attractive but significantly weaker.

In the present work we investigate by resistivity recovery measurements the interaction between carbon atoms and radiation defects in Fe - 11 at. % Cr alloys, which are considered as model materials for the more complex ferritic/martensitic steels with Cr concentration in the range 9–12 wt. %. This steel grade is of crucial importance for nuclear applications and it is currently considered as structural material for future energy generating fusion reactors [5] primarily due to its superior resistance to radiation damage accumulation and swelling. However, there are still issues that have to be resolved as, e.g, the low temperature irradiation embrittlement. Further development and study of these materials are currently undertaken and the interaction of radiation defects with solute atoms as carbon is of particular interest since it may play a key role in the irradiation performance of these steels.

The measurement of electrical resistivity is a very sensitive and reliable method for the study of irradiation defects. The residual resistivity of an irradiated metallic specimen increases by an amount proportional to the defect concentration. If the irradiation is performed at a sufficiently low temperature defect migration is inhibited and by monitoring the recovery of the resistivity as a function of temperature during post-irradiation annealing information can be obtained on defect reaction kinetics. For example the resistivity of pure iron irradiated at liquid helium temperature displays a sharp drop during annealing at around 100 K due to the onset of self-interstitial atom (SIA) migration and the associated vacancy-SIA recombination reactions [2]. This is the temperature range of the so-called recovery stage I. Detailed studies of resistivity recovery in stage I provided significant information on the properties of SIAs in iron [2].

Measurements of resistivity recovery in concentrated Fe–Cr alloys with Cr concentrations comparable to ferritic/martensitic steels have been previously reported in [6–9] and several theoretical works [10–13] have discussed the relevant point defect properties in correlation with the experimental results. The main findings and their interpretation are briefly summarized here. Stage I recovery is still observed in the concentrated alloys at roughly the same

* Corresponding author.
E-mail address: gapost@ipta.demokritos.gr (G. Apostolopoulos).

http://dx.doi.org/10.1016/j.nme.2016.09.007

Table 1
Concentrations of alloying elements in Fe–Cr alloys (at.%).

Alloy Code	Cr	C	Other Impurities (O, N, P)
Fe-11Cr	10.8	0.002	0.004
Fe-11Cr–C	10.7	0.380	0.004

temperature range as in iron. However, its amplitude is strongly suppressed with increasing Cr concentration and its peak is shifted towards lower temperatures. The former of these two effects has been attributed to trapping of self-interstitial defects by Cr atoms whereas the latter to the higher mobility of mixed (Fe–Cr) interstitial dumbbells that occur with increasing Cr concentration. At higher temperatures the stages II (150–200 K) and III (200–250 K) are observed which also bear similarity to the corresponding recovery stages in pure Fe. In the pure metal these stages are associated with the migration of di-interstitials and vacancies, respectively. In the alloy the proposed interpretations are different. According to recent detailed calculations [13], the appearance of stage II is due to the detrapping of SIA defects while stage III is due to vacancy migration which is not significantly affected by Cr. However, other authors suggest that correlated vacancy recombination may be responsible for recovery features in stage II while SIAs are released from Cr traps at temperatures close to stage III [7,9].

In the present work we employ proton irradiation at cryogenic temperatures to introduce radiation defects in an Fe–11 at.% Cr alloy and a similar alloy doped with carbon. *In-situ* measurements of the electrical resistivity are utilized for assessing the associated radiation damage and its recovery during subsequent post-irradiation annealing. The effect of carbon on point defect properties is revealed by comparing the resistivity recovery of carbon-doped and undoped Fe–Cr alloy.

2. Experimental methods

The starting materials were two high purity alloys obtained from EFDA[1] with the composition shown in Table 1 as determined by chemical analysis. Both alloys contain about 11 at. % Cr while one of them is doped with C to a concentration of 0.38 at. %. They will be referred as Fe–11Cr and Fe–11Cr–C for the undoped and carbon-doped case, respectively. These materials were developed as model alloys with Cr and C concentration similar to that of ferritic/martensitic steels. They have been prepared by induction melting under high purity hydrogen and argon to reduce foreign impurities to the levels shown in Table 1. The residual carbon content in Fe–11Cr is approximately 20 appm.

Both alloys were supplied as cylindrical bars of 10 mm diameter. Fe–11Cr was in the recrystallized state with a final annealing of 1 h at 800 °C under argon flow followed by air cooling. Fe–11Cr–C was austenitized for 1 h at 940 °C with subsequent air cooling followed by 1 h tempering at 760 °C and air cooling.

Specimens in the form of 50 μm thick foils were prepared by cold-rolling of thin (~300 μm) wafers cut from the bars by means of a diamond saw. The specimens were chemically cleaned after each metallurgical step and finally electropolished to their final thickness. To relieve the effects of cold-working the Fe–11Cr foils were annealed for 12 h at 800 °C under a hydrocarbon-free vacuum of 10^{-6}mbar while the carbon doped ones were annealed for 1 h at 760 °C under the same vacuum conditions. After annealing the samples were quickly removed from the furnace. Due to the small specimen mass the cooling rate is equivalent to air cooling of the bulk alloys.

[1] European Fusion Development Agreement.

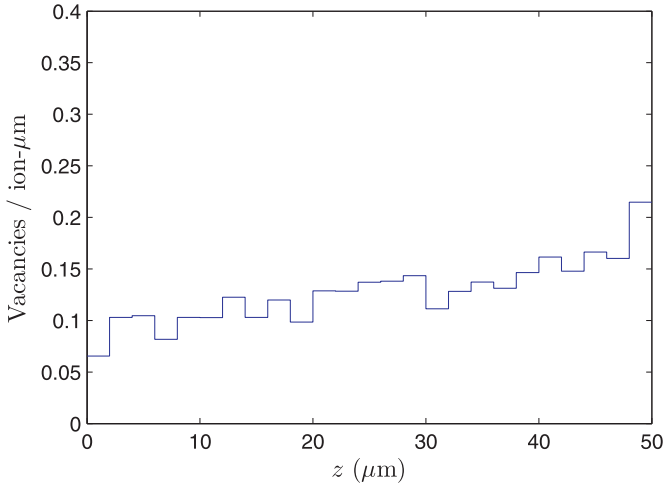

Fig. 1. Profile of the damage generated in the Fe-11Cr alloy foil specimens as a function of depth during irradiation by 5 MeV protons.

Inspection by optical microscopy showed that Fe–11Cr exhibits a ferritic microstructure with large grains of ~100 μm average size. On the other hand the carbon doped Fe–11Cr–C displays the characteristic tempered martensitic microstructure which is typical of 9–12%Cr ferritic/martensitic steels containing similar concentrations of carbon and subjected to a similar heat treatment [14,15]. It is well known that part of the C in these materials precipitates in the form of chromium/iron $M_{23}C_6$ carbides after tempering [14,15] and this is also expected to be the case in Fe–11Cr–C. The amount of carbon that remains in solid solution in the matrix is expected to be of the order of the solubility at the annealing temperature, i.e. approx. ~1000 at. ppm.

Current and potential leads of pure Fe were spot-welded on the specimens for performing the electrical resistivity measurements according to the standard DC four-probe method using a constant current source and a sensitive nano-voltmeter (Keithley Inc). Current polarity reversal was used to eliminate thermal voltages. The resolution of the measurement system was $10^{-7}\Omega$.

Irradiations were performed in the dedicated materials irradiation facility IR[2] at the TANDEM accelerator of NCSR "Demokritos" [16], which offers the capability for *in-situ* measurement of the electrical resistivity during and after irradiation. The samples were irradiated by a beam of 5 MeV protons, which have a projected range of approx. 80 μm in iron as obtained from the ion range tables provided by the software SRIM [17]. Thus the energetic protons penetrate fully the 50 μm foil specimens. A detailed ion transport simulation by means of SRIM [17] results in the damage profile shown in Fig. 1 in terms of vacancies generated per ion and per unit length. As it is seen from the figure the damage profile is fairly flat and thus defects are generated almost homogeneously within the irradiated volume. The simulation shows also that the number of implanted protons in the specimen is 4 orders of magnitude lower than the corresponding number of generated vacancies. The total damage in displacements per atom (dpa) as calculated by SRIM, averaged over the sample thickness, is given in Table 2 together with the proton flux and maximum fluence utilized in the irradiations.

During irradiation the sample temperature was kept at 50 K by a closed-cycle helium refrigerator coupled to the accelerator beam line. At specific time intervals during the irradiation the proton beam was closed, the sample was cooled down to 20 K and its irradiation induced residual resistivity increase was measured. In this manner the damage generation could be monitored as a function of dose. The total resistivity increase corresponding to the maxi-

Table 2
Conditions of the 5 MeV proton irradiation.

	Φ (cm^{-2} s^{-1})	$[\Phi \cdot t]_{max}$ (cm^{-2})	Total Damage (dpa)	ρ_i^0 ($\mu\Omega$-cm)
Fe-11Cr	2.0×10^{11}	2.7×10^{15}	3.8×10^{-5}	0.57 ± 0.03
Fe-11Cr–C	1.8×10^{11}	3.1×10^{15}	4.3×10^{-5}	0.66 ± 0.03

Φ - beam flux; $\Phi \cdot t$ - fluence; ρ_i^0 - max. irradiation induced resistivity increase.

mum dose is given in Table 2. Recovery annealing up to 700 K was performed *in-situ* without removing the sample from the irradiation chamber. The annealing temperature was increased in steps ΔT keeping a constant ratio $\Delta T/T \approx 0.03$. At each temperature step the annealing time Δt was such that $\Delta T/\Delta t = 1$ K/min. At the end of each annealing interval the sample was rapidly quenched to the base temperature of 20 K and the residual resistivity was measured. Thus the resistivity recovery was measured as a function of annealing temperature.

3. Damage generation

The irradiation induced increase of the electrical resistivity ρ_i is shown in Fig. 2a as a function of dose for both the pure and C-doped samples. The observed almost linear increase is due to the accumulation of radiation defects since at the irradiation temperature of 50 K their mobility is significantly reduced and thus there is a low likelihood for annihilation to occur. From Fig. 2a it is deduced that carbon does not have a significant effect on the damage generation. The experimental curves in Fig. 2a deviate slightly from a pure linear increase. This is more clearly seen in Fig. 2b, where the resistivity damage rate $\Delta\rho_i/\Delta[\Phi \cdot t]$ is depicted as a function of dose. The damage rate data of Fig. 2b are obtained by a point-by-point differentiation of the resistivity versus dose curves. The damage rate as a function of dose is well described by a linear relationship $a + b\,\Phi \cdot t$, where a and b are constants, which is depicted with the dotted line in Fig. 2b. The parameter a expresses the initial damage rate at zero dose and b quantifies the gradual decrease of damage rate. The best-fit values for the parameters are $a = (2.2 \pm 0.2) \times 10^{-22}\Omega$-cm^3 and $b = -(6 \pm 1) \times 10^{-39}\Omega$-cm^5, respectively. It is noted that the damage rate at the end of the irradiation is 10% lower than the initial one.

For a proper estimation of the amount of damage generated by the proton irradiation the results of the SRIM simulations of Section 2 have been processed according to the recommendations of Stoller et al. [18]. In brief, the average damage energy T_{dam} is obtained from the SRIM output and then this value is inserted in the NRT model of displacement damage [19] to estimate the number of atomic displacements. A displacement threshold energy of $T_d = 40$ eV has been used, which is the value typically used for Fe [20]. The SRIM simulation predicts an average damage energy per displacement collision event, $T_{dam} = 300$ eV. Thus, according to the NRT model a number of $0.8T_{dam}/2T_d = 3$ Frenkel pairs are generated per collision. Taking also into account the number of displacement collisions per ion from SRIM, the value of the damage cross section is found equal to $\sigma_d = 1.4 \times 10^{-20}$cm^2. Due to the low damage energy T_{dam} most of the collisions would result in the production of isolated Frenkel pairs and only a small fraction of defects will form larger clusters. Recent molecular dynamics simulations of displacement cascades in iron [21] suggest that at this level of damage energy the fraction of interstitials in clusters would be of the order of 20% while for the vacancies a smaller fraction is anticipated.

The resistivity damage rate is equal to $\rho_F\sigma_d$, where ρ_F is the resistivity per unit concentration of Frenkel defects. Equating this to the experimental initial damage rate a it is obtained that the apparent value of ρ_F is $(1.6 \pm 0.2) \times 10^{-2}\Omega$-cm in both undoped and C-doped Fe–11 at.% Cr. Compared to the Frenkel pair resistivity of pure Fe $\rho_F(\text{Fe}) = (3.0 \pm 0.5) \times 10^{-3}\Omega$-cm [22] the value obtained here is 5 times higher. This is in agreement with previous results of Maury et al. [23] who observed an up to 6-fold increase of ρ_F in electron irradiated Fe–Cr alloys with a maximum Cr concentration of 3 at.%. These authors attributed the effect to the non-additivity of different conduction electron scattering mechanisms contributing to the total resistivity. This is also known as deviations from Matthiessen's rule and in ferromagnetic Fe alloys it is mainly due to spin dependent electron scattering. In the case of irradiated Fe–Cr the scattering of conduction electrons from Frenkel defects and Cr atoms has different intensity in the spin-up and spin-down bands. This may account for the observed increase in the apparent resistivity per Frenkel defect found here and in [23].

Regarding the observed decrease of the damage rate with dose it can be either due to radiation annealing, i.e., the annihilation of already present radiation defects by the new collisions occurring in their vicinity, or to the effects of spin dependent conduction discussed in the previous paragraph. Similar observations of diminishing damage rate in [23] have been attributed to deviations from

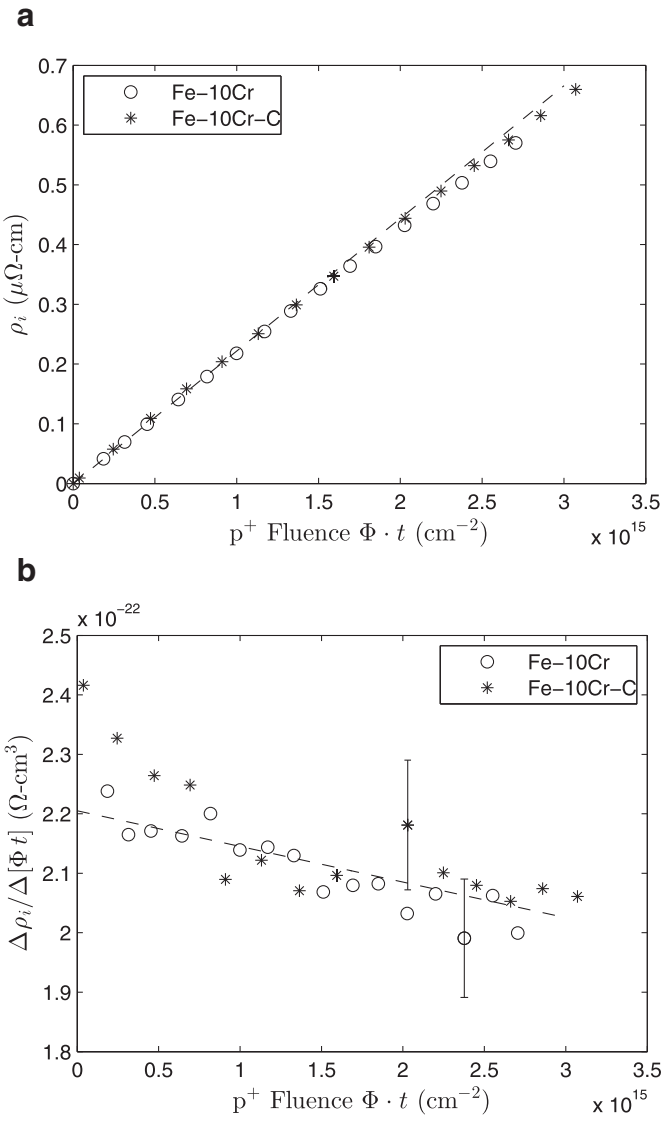

Fig. 2. (a) Irradiation induced residual resistivity increase ρ_i and (b) resistivity damage rate as a function of dose in undoped and C-doped Fe–Cr alloys during proton irradiation at 50 K.

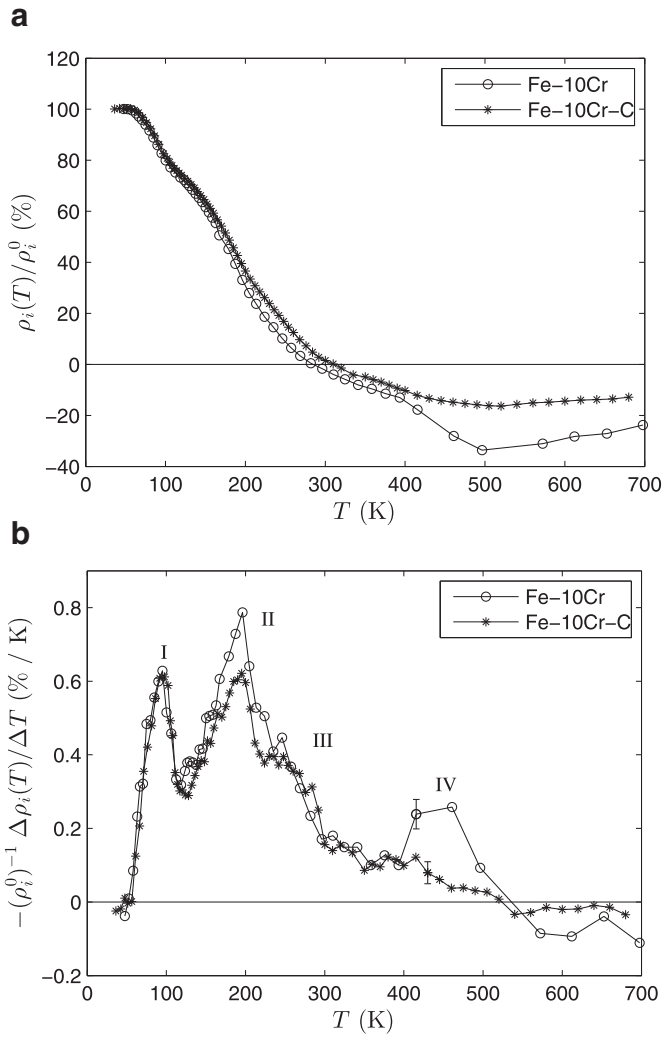

Fig. 3. (a) Resistivity recovery and (b) recovery rate as function of annealing temperature for C-doped and undoped Fe–Cr alloys after proton irradiation at 50 K.

Matthiessen's rule by Maury et al. However, the effect of radiation annealing cannot be excluded. Experimental data extending to sufficiently higher dose would be needed in order to discriminate between these two effects.

4. Resistivity recovery

Fig. 3a shows the resistivity recovery of Fe–11Cr and Fe–11Cr–C alloys as a function of annealing temperature. The ratio $\rho_i(T)/\rho_i^0$, where $\rho_i(T)$ is the remaining resistivity at temperature T, reflects the fraction of radiation defects that survive after annealing at the given temperature. It is observed that the recovery proceeds similarly in the two materials, however the presence of carbon slows down the recovery process in the Fe–11Cr–C alloy above about 200 K. Notably, in both materials the resistivity recovery becomes negative above 300 K, i.e., the resistivity of the samples becomes lower than their pre-irradiation value. Such reduction of resistivity in irradiated and annealed concentrated alloys has been frequently observed in the past [24,25] and was typically attributed to solute atom re-ordering taking place during the migration of remaining radiation defects. The effect is more pronounced in the Fe–11Cr alloy. It is noted that this effect is observed in the present experiments only during post-irradiation annealing. Annealing of un-irradiated Fe–11Cr and Fe–11Cr–C samples in the temperature range 300–600 K does not result in significant changes of the residual resistivity. Thus the observed resistivity reduction above 300 K must be associated with the annealing of radiation defects.

Table 3
Resistivity recovery stage data.

Stage		Fe-11Cr	Fe-11Cr–C
I	$\hat{T}$(K)	95 ± 3	95 ± 3
	A (%)	27 ± 2	27 ± 2
II	$\hat{T}$(K)	195 ± 5	195 ± 5
	A (%)	50 ± 3	42 ± 3
III	$\hat{T}$(K)	240 ± 5	250 ± 5
	A (%)	30 ± 3	33 ± 3
IV	$\hat{T}$ (K)	440 ± 10	400 ± 10
	A (%)	28 ± 2	11 ± 2

$\hat{T}$: Temperature of the maximum in the recovery rate; A: total resistivity recovery

In fig. 3b the recovery rate $-(\rho_i^0)^{-1}\Delta\rho_i(T)/\Delta T$ is presented as a function of annealing temperature. $\Delta\rho_i(T)=\rho_i(T)-\rho_i(T-\Delta T)$ represents the difference in remaining resistivity between two successive annealing temperatures separated by ΔT. The graph of the recovery rate assists in the identification of temperature regions of fast recovery that may be associated with different defect reactions. The curves in Fig. 3b show four distinct maxima, or recovery stages, labeled from I to IV. The temperature of the maximum $\hat{T}$ (K) and the total recovery A (%) associated with each stage are listed in Table 3. The quantity A represents the integrated area beneath a recovery peak in Fig. 3b and it is associated with the percentage of defects annealed in the temperature range defined from the start to the end of the peak.

The effect of carbon on the resistivity recovery is more clearly revealed in fig. 3b where it is observed that carbon affects mainly stages II and IV. There is no effect of C on stage I and only a slight influence on stage III. In the next paragraphs we discuss the effect of carbon on the recovery stages based on the current understanding of recovery processes in Fe–Cr from previous experimental [6–8,23] and theoretical [11,13,26] work.

We have to take also into account that due to the presence of C, Fe–11Cr–C exhibits a significantly different microstructure and this in turn may affect the recovery. To compare the relative contribution of microstructure features to point defect migration in the Fe–11Cr–C samples we estimate the associated sink strength k^2 according to [27], ch. 5. This quantity offers a description of the tendency of various sinks to absorb point defects independent of the point defect migration velocity and concentration. For the interaction of mobile point defects with carbon atoms in solid solution the sink strength is given by $k_C^2 = 4\pi R_C[C]$ where R_C is the carbon/point defect interaction radius and $[C]$ the carbon volume concentration. For typical values of $R \sim 4a_{Fe}$ [2], where a_{Fe} is the iron lattice constant, and carbon concentration equal to the solubility (~1000 ppm) we obtain $k_C^2 \sim 10^{14}\text{cm}^{-2}$. For point defect loss to grain boundaries the sink strength is $k_{GB}^2 \approx 24/d^2$, where d is the grain size. The characteristic laths of the martensitic microstructure exhibit typical widths of $d \sim 500$nm [28] thus we obtain $k_{GB}^2 \sim 10^{10}\text{cm}^{-2}$. Regarding the carbide precipitates, their sink strength is given by $k_p^2 = 4\pi R_p\rho_p$,[2] where R_p and ρ_p are the radius and volume density of precipitates, respectively. With an average $R_p \sim$ 100nm and $\rho_p \sim 10^{13}\text{cm}^{-3}$ [14,15] it is obtained that $k_p^2 \sim 10^9\text{cm}^{-2}$. Finally, dislocations present a sink strength $k_d^2 = 2\pi\rho_d/\ln(\mathcal{R}/R_d)$‡ where ρ_d is the dislocation line density, $\mathcal{R}$ is the mean distance between dislocations and R_d is the dislocation/point defect interaction radius. It is known that ferrous martensites ex-

[2] We are in the regime of diffusion controlled reactions (cf. [27]).

hibit high dislocation densities up to $\rho_d \sim 10^{12}\text{cm}^{-2}$ [28]. Setting $R_d \sim 4a_{Fe}$ and $\mathcal{R} \sim \rho_d^{-2}$ it is obtained that $k_d^2 \sim 4 \times 10^{12}\text{cm}^{-2}$. Comparing the sink strength of the various mechanisms it is seen that carbon in solid solution is the most important for point defect migration. The presence of dislocations may also play a role, while the contribution from grain boundaries and carbide precipitates is relatively much smaller.

It is also noted that our discussion of the recovery will be largely based on considerations relating to isolated Frenkel pairs The possible effects of small defect clusters that may form during proton irradiation will not be considered. This is justified by the relatively small number of such clusters (at most 20% of the total defect number) [29] and by the fact that the measured resistivity recovery of proton irradiated Fe–11Cr is very similar to previous results obtained on Fe–Cr alloys with a similar Cr concentration and irradiated with electrons [6]. This similarity is explicitly indicated in the following paragraphs in relation to the various recovery stages.

Stage I. This stage is attributed to the correlated recombination of Frenkel defects by the migration of self-interstitial atoms (SIA) to their corresponding near lattice vacancies. In comparison to pure Fe this stage in concentrated Fe–Cr alloys is observed at lower temperature and with significantly reduced amplitude. The present results regarding the temperature position and height of the recovery peak are in agreement with previous experimental results [6,8] obtained after electron irradiation of alloys with similar Cr concentration. The behavior of stage I has been attributed by several authors [8,11,13] to the trapping of SIAs by Cr atoms. In Fe–11Cr–C despite the high carbon concentration there is no observed effect of the carbon atoms on the correlated recovery stage although it is known that C impurities may also act as traps for interstitial defects in Fe [2]. Apparently the trapping of interstitials mainly takes place by Cr which is to be expected taking into account the much higher concentration of Cr with respect to C.

Stage II. This stage has been attributed [13] to the release of SIA defects captured by Cr during stage I migration. According to [13], the SIA-trap dissociation energy is 0.45 eV The interstitials are detrapped at higher temperature leading to the occurrence of stage II in the temperature range 150–200 K. The maximum of stage II is observed here at $\hat{T} = 195\text{K}$, both in the undoped and C-doped alloys, in agreement with previous observations in Fe–Cr alloys of similar concentration [6]. However, the presence of C has a significant effect on the total recovery in stage II, which is reduced by about 10% (cf. Table 3). This may be explained by assuming that a fraction of the SIAs released from Cr traps during stage II are re-trapped by C atoms. The associated dissociation energy of the carbon-SIA complex should be higher than 0.45 eV in order to survive stage II recovery. Experiments [2] and recent theoretical calculations [30] predict a low binding energy of such complexes in pure Fe, therefore, the higher dissociation energy of carbon-SIA complexes assumed here could be attributed either to an increase in the carbon-SIA binding energy due to the presence of Cr in the matrix or to the occurrence of complex defect configurations. Alternatively one might assume that the reduction of stage II in Fe–Cr–C is due to absorption of SIA defects by the increased concentration of defect sinks that is present in this material due to its microstructure. However, as discussed above, the effect of these sinks on SIA migration is expected to be relatively small and cannot explain the large reduction of stage II. This is further supported by the fact that stage III, which is also most probably due to long range migration of point defects (see below), remains almost unchanged in Fe–11Cr–C despite the microstructural differences.

Stage III has been generally associated with vacancy migration, both in Fe–Cr alloys [6,13] as well as in pure Fe [2]. The stage is observed here in the same temperature range as in previous work in electron irradiated Fe–Cr [6]. From Fig. 3b it is seen that the presence of C in Fe–11Cr–C does not seem to have a significant effect on the recovery in stage III. This is surprising since according to several works [1–4] there is a strong interaction between vacancies and carbon atoms in Fe and it would be expected that this interaction is also present in Fe–Cr alloys. In the resistivity recovery of pure Fe, C has a significant effect on stage III; the stage is shifted to lower temperature and the reaction kinetics changes from 2nd order to 1st order [2]. According to Takaki et al. [2] this is attributed to the capture of the diffusing vacancies by carbon atoms. Essential for this interpretation is also that the specific resistivity of the vacancy-carbon (V-C) complex must be lower than the sum of the resistivities of the individual isolated defects. However, there are no theoretical calculations to back up this assumption. In the present experiments, only a small shift of the stage can be observed in the C-doped alloy and this is towards higher temperature, i.e., in the opposite direction with respect to the results in [2]. The present results could be understood by estimating the concentration of vacancies present before stage III. This is about 8 ppm taking into account the initial defect concentration of 40 ppm (see above) and the total recovery in the previous stages (cf. Table 3). Comparing the vacancy concentration before stage III to the residual C content present already in the undoped Fe–11Cr alloy it is seen that they are of the same order of magnitude. Thus it could be assumed that already in the undoped Fe–11Cr there is significant interaction between vacancies and carbon and this is why the much higher C concentration present in the Fe–11Cr–C alloy does not lead to large observable effects in stage III. However, this does not explain the small shift of the stage towards higher temperature observed in the C-doped alloy. It is noted here that theoretical calculations of the resistivity contributions from different defects and defect complexes would be very helpful in order to clarify such issues.

Stage IV. This stage is clearly related to solute atom re-ordering effects since a large part of the negative recovery is developed within the temperature range of this stage, 400–500 K (cf. Fig. 3a). At the annealing temperature of 500 K the fractional resistivity reduction is equal to −34 and −16% in Fe–11Cr and Fe–11Cr–C, respectively. A similar resistivity reduction of approx. −10 % has been previously observed in an Fe–Cr alloy with Cr concentration close to 10 at. % after electron irradiation and annealing up to 300 K [7]. However, a clear recovery stage has not been previously measured. Fe–Cr is known to exhibit short-range ordering at concentrations below about 10 at.% and short-range clustering above this concentration [31,32]. Furthermore, it has been observed that the resistivity of unirradiated Fe–10 at.% Cr is slightly reduced during annealing at temperatures above 700 K due to the re-ordering of solute atoms. This resistivity reduction becomes more pronounced at higher Cr concentration where short-range clustering of Cr occurs [31]. Thus, the resistivity reduction observed here is attributed to weak short-range clustering of Cr atoms that occurs via the dissociation and migration of irradiation defects in stage IV. The defects involved in stage IV could be most probably identified as the ones that form during stage III, i.e., small vacancy clusters and V-C complexes. Thus, in Fe–11Cr stage IV could be attributed to the dissociation of vacancy or V-C complexes and the associated migration of released point defects. Such a process is known to occur in pure Fe at 500 K but may be shifted to lower temperatures in Fe–Cr due to a reduction of the binding energy of the defect complexes. The released vacancies in the matrix assist the diffusion (radiation enhanced diffusion) of the Cr resulting to its clustering. The suppression of stage IV in the C-doped alloy could be due to several reasons. First, the martensitic microstructure of Fe–11Cr–C may hinder the reordering of Cr. Changes in alloy ordering require long range point defect migration which may not be possible due to the presence of high concentration of defect sinks in this material. Alter-

natively, since C is also mobile in this temperature range, it may interact with V-C to form V-C_2 complexes. Theoretical calculations show that in Fe these are more stable than V-C [3,4]. Thus in Fe–11Cr–C a number of vacancies could remain bound in V-C_2 complexes which results in a reduction of Cr enhanced diffusion and subsequently in less Cr clustering.

5. Conclusion

The interaction of carbon with irradiation defects has been studied in Fe–Cr alloys with an 11 at.% concentration of Cr. Samples of this alloy doped with 0.38 at.% of carbon as well as undoped were irradiated at 50 K with 5 MeV protons. The effect of carbon was revealed by comparing the resistivity recovery of undoped and C-doped alloys measured during post-irradiation annealing. It was observed that the presence of carbon affects mainly the stages II and IV of the recovery spectrum. The reduction of the recovery in stage II is attributed to trapping of migrating self-interstitial defects by carbon atoms. Stage IV is attributed to short-range Cr clustering occurring during the dissociation and migration of irradiation defects. These defects are identified as vacancy or vacancy-carbon clusters. The presence of C suppresses the occurrence of stage IV.

Acknowledgments

The authors would like to thank the TANDEM accelerator operators M. Adrianis and V. Andreopoulos and also E. Tsopanakis for assistance during the irradiation experiments. This work was carried out within the EUROfusion Consortium and received funding from the Euratom research and training programme 2014–2018 under grant agreement number No 633053. The views and opinions expressed herein do not necessarily reflect those of the European Commission. Furthermore, the authors acknowledge funding from the Greek General Secretariat for Research and Technology and the European Regional Development Fund under the Action “Development Grants For Research Institutions–KRIPIS” of OPCE II.

References

[1] A. Vehanen, P. Hautojärvi, J. Johansson, J. Yli-Kauppila, P. Moser, Vacancies and carbon impurities in α-iron: Electron irradiation, Phys. Rev. B 25 (2) (Jan. 1982) 762–780.
[2] S. Takaki, J. Fuss, H. Kuglers, U. Dedek, H. Schultz, The resistivity recovery of high purity and carbon doped iron following low temperature electron irradiation, Radiat. Eff. Defects Solids 79 (1) (1983) 87–122.
[3] C. Domain, C.S. Becquart, J. Foct, Ab initio study of foreign interstitial atom (C, N) interactions with intrinsic point defects in α-Fe, Phys. Rev. B 69 (14) (2004) 144112.
[4] C.C. Fu, E. Meslin, A. Barbu, F. Willaime, V. Oison, Effect of C on vacancy migration in α-iron, in *Solid State Phenomena* 139 (2008) 157–164.
[5] D. Stork, P. Agostini, J.-L. Boutard, D. Buckthorpe, E. Diegele, S.L. Dudarev, C. English, G. Federici, M.R. Gilbert, S. Gonzalez, A. Ibarra, C. Linsmeier, A.L. Puma, G. Marbach, L.W. Packer, B. Raj, M. Rieth, M.Q. Tran, D.J. Ward, S.J. Zinkle, Materials R&D for a timely DEMO: Key findings and recommendations of the EU Roadmap Materials Assessment Group, Fusion Eng. Des. 89 (7–8) (Oct. 2014) 1586–1594.
[6] A. Benkaddour, C. Dimitrov, O. Dimitrov, Irradiation-Induced Defects in Ferritic FeCr Alloys, in *Materials Science Forum* 15 (1987) 1263–1268.
[7] A.L. Nikolaev, V.L. Arbuzov, A.E. Davletshin, On the effect of impurities on resistivity recovery, short-range ordering, and defect migration in electron-irradiated concentrated Fe - Cr alloys, J. Phys. Condens. Matter. 9 (21) (May 1997) 4385.
[8] A.L. Nikolaev, Stage I of recovery in 5 MeV electron-irradiated iron and iron-chromium alloys: the effect of small cascades, migration of di-interstitials and mixed dumbbells, J. Phys. Condens. Matter. 11 (44) (Nov. 1999) 8633.
[9] A. Nikolaev, Specificity of stage III in electron-irradiated Fe-Cr alloys, Philos. Mag. 87 (31) (2007) 4847–4874.
[10] T.P.C. Klaver, P. Olsson, M.W. Finnis, Interstitials in FeCr alloys studied by density functional theory, Phys. Rev. B 76 (21) (Dec. 2007) 214110.
[11] D. Terentyev, P. Olsson, T.P.C. Klaver, L. Malerba, On the migration and trapping of single self-interstitial atoms in dilute and concentrated Fe-Cr alloys: Atomistic study and comparison with resistivity recovery experiments, Comput. Mater. Sci. 43 (4) (2008) 1183–1192.
[12] P. Olsson, Ab initio study of interstitial migration in Fe–Cr alloys, J. Nucl. Mater. 386–388 (Apr. 2009) 86–89.
[13] D. Terentyev, N. Castin, C.J. Ortiz, Correlated recombination and annealing of point defects in dilute and concentrated Fe–Cr alloys, J. Phys. Condens. Matter 24 (47) (Nov. 2012) 475404.
[14] K. Mergia, N. Boukos, Structural, thermal, electrical and magnetic properties of Eurofer 97 steel, J. Nucl. Mater. 373 (1–3) (Feb. 2008) 1–8.
[15] P. Fernández, A.M. Lancha, J. Lapeña, M. Hernández-Mayoral, Metallurgical characterization of the reduced activation ferritic/martensitic steel Eurofer'97 on as-received condition, Fusion Eng. Des. (58–59) (Nov. 2001) 787–792.
[16] G. Apostolopoulos, Fusion Technology Group - IR^2. http://www.ipta.demokritos.gr/ftg/ir2.html, 2011.
[17] J.F. Ziegler, M.D. Ziegler, J.P. Biersack, SRIM – The stopping and range of ions in matter (2010), Nucl. Instrum. Methods Phys. Res. Sect. B Beam Interact. Mater. At. 268 (11–12) (Jun. 2010) 1818–1823.
[18] R.E. Stoller, M.B. Toloczko, G.S. Was, A.G. Certain, S. Dwaraknath, F.A. Garner, On the use of SRIM for computing radiation damage exposure, Nucl. Instrum. Methods Phys. Res. Sect. B Beam Interact. Mater. At. 310 (Sep. 2013) 75–80.
[19] M.J. Norgett, M.T. Robinson, I.M. Torrens, A proposed method of calculating displacement dose rates, Nucl. Eng. Des. 33 (1) (Aug. 1975) 50–54.
[20] P. Jung, Average atomic-displacement energies of cubic metals, Phys. Rev. B 23 (2) (Jan. 1981) 664–670.
[21] R.E. Stoller, 1.11 Primary Radiation Damage Formation, Comprehensive Nuclear Materials, Elsevier, Oxford, 2012, pp. 293–332.
[22] F. Maury, M. Biget, P. Vajda, A. Lucasson, P. Lucasson, Anisotropy of defect creation in electron-irradiated iron crystals, Phys. Rev. B 14 (12) (Dec. 1976) 5303–5313.
[23] F. Maury, P. Lucasson, A. Lucasson, F. Faudot, J. Bigot, A study of irradiated FeCr alloys: deviations from Matthiessen's rule and interstitial migration, J. Phys. F Met. Phys. 17 (5) (1987) 1143–1165.
[24] P. Vaessen, B. Lengeler, W. Schilling, Recovery of the electrical resistivity in electron-irradiated, concentrated silver-zinc alloys, Radiat. Eff. 81 (3–4) (Jan. 1984) 277–292.
[25] E. Balanzat, J. Hillairet, A quench and irradiation study of the vacancy parameters in alpha -Cu-30 at% Zn, J. Phys. F Met. Phys. 11 (10) (Oct. 1981) 1977.
[26] C.J. Ortiz, D. Terentyev, P. Olsson, R. Vila, L. Malerba, Simulation of defect evolution in electron-irradiated dilute FeCr alloys, J. Nucl. Mater. 417 (1–3) (Oct. 2011) 1078–1081.
[27] G.S. Was, Fundamentals of radiation materials science: metals and alloys, Springer Science & Business Media, 2007.
[28] H. Bhadeshia, R. Honeycombe, Steels: microstructure and properties, Butterworth-Heinemann, 2006.
[29] R.E. Stoller, G.R. Odette, B.D. Wirth, Primary damage formation in bcc iron, J. Nucl. Mater. 251 (Nov. 1997) 49–60.
[30] T. Jourdan, C.C. Fu, L. Joly, J.L. Bocquet, M.J. Caturla, F. Willaime, Direct simulation of resistivity recovery experiments in carbon-doped α-iron, Phys. Scr. 2011 (T145) (Dec. 2011) 14049.
[31] I. Mirebeau, M. Hennion, G. Parette, First Measurement of Short-Range-Order Inversion as a Function of Concentration in a Transition Alloy, Phys. Rev. Lett. 53 (7) (Aug. 1984) 687–690.
[32] I. Mirebeau, G. Parette, Neutron study of the short range order inversion in $Fe_{1-x}Cr_x$, Phys. Rev. B 82 (10) (Sep. 2010) 104203.